RESEARCH ARTICLE

The role of the Agulhas in the Benguela Current system: A numerical modeling approach

Jennifer A. Veitch[1,2] (ID) and Pierrick Penven[3] (ID)

[1]South African Environmental Observation Network, Egagasini Node, Private Bag X2, Roggebaai, South Africa, [2]Department of Oceanography, University of Cape Town, Cape Town, South Africa, [3]Laboratoire des Physique des Océans (UMR 6523 CNRS, IFREMER, IRD, UBO), Brest, France

Key Points:
- ~15 Sv of the mean Benguela Current is of Agulhas origin and its meandering nature a result of the path of Agulhas Rings
- Shelf-edge jets are driven by intense density fronts and are enhanced by Agulhas influx and dynamic uplift via vortex squashing
- High turbulence is tied to shelf-edge jets and large filaments at the perennial Luderitz upwelling cell

Correspondence to:
J. A. Veitch,
veitch.jennifer@gmail.com

Abstract A modeling approach is used to investigate the influence of the Agulhas on the southern Benguela system. Two climatological ROMS simulations are run that are identical except that in one of them the effect of the Agulhas is removed. Comparing their outputs allows for a clear indication of the role of the Agulhas on both the large-scale and shelf dynamics. About 15 Sv of the mean transport of the Benguela Current is shown to be contributed by Agulhas influx, with the most intense flow being associated with extreme turbulence and its meandering nature is a reflection of the passage of Agulhas Rings. The injection of warm water is particularly evident beyond the shelf-edge, producing a perennially intense cross-shelf density front that is enhanced during upwelling season. This gradient drives a jet that is fastest at the shelf-edge but that extends from the midshelf to at least 100 km beyond it and is associated with dynamic uplift via vortex squashing. Similarly generated is the Good Hope Jet that extends northwestward from the western Agulhas Bank. Turbulence associated with Agulhas leakage increases rapidly beyond the shelf-edge causing the upwelling front in the southern Benguela to be subject to intense mixing, leaving a relatively uniform front there. Locally generated regions of high turbulence exist in the vicinity of the shelf-edge jets as well as further north in association with the large filaments that originate from the perennial Lüderitz upwelling cell, with or without the influence of the Agulhas.

1. Introduction

The Benguela system is unique as one of the world's four major eastern boundary upwelling systems due to its proximity to a western boundary current, namely the Agulhas Current. Rings, eddies, and filaments that spawn at the Agulhas retroflection therefore have a significant influence on the mean state and mesoscale variability of the Benguela system. The review chapter by *Capet et al.* [2008] on eddies in eastern boundary current systems (EBCS) provides an excellent impression of the present state of our understanding of the role of eddies in EBCSs and also points out the unusual nature of the Benguela Current system. In this work, the Benguela system refers to both the Benguela Current, which is the eastern limb of the south Atlantic subtropical gyre, and the nearshore Benguela upwelling regime and its associated dynamics.

The transport of the Benguela Current across 30°S has been estimated to be approximately 20–25 Sv [*Peterson and Stramma*, 1991]. However, time series data obtained from the 1992–1993 BEST (Benguela Sources and Transport) monitoring campaign suggest that this is only the case when an Agulhas Ring is present [*Garzoli et al.*, 1996] and that the annual mean transport is closer to 16 Sv. The large disparity in these transport estimates is evidence of the huge impact the Agulhas has on the Benguela Current. Agulhas leakage into the Atlantic ocean via the Benguela Current through the Agulhas eddy corridor [*Garzoli and Gordon*, 1996] is thought to be pivotal to Indian-Atlantic exchange of heat and salt, which is a key component of the global thermohaline circulation pattern [*Gordon*, 2003; *Biastoch et al.*, 2008a]. Its global significance has thus led to much effort being placed on quantifying the so-called Agulhas "leakage" by identifying what portion of the Benguela Current transport originates from the Indian Ocean. Direct observations have estimated Agulhas leakage to be between 2 and 10 Sv [*de Ruijter et al.*, 1999] and both Eulerian [*Reason et al.*, 2003; *Matano and Beier*, 2003; *van Sebille et al.*, 2010; *Loveday et al.*, 2014, 2015] and Lagrangian [*Doglioli et al.*, 2006; *van Sebille et al.*, 2010; *Biastoch et al.*, 2008b; *Durgadoo et al.*, 2013] approaches have been used to estimate the leakage from models and tend to be in the 10–20 Sv range. *Biastoch et al.* [2008b] compared leakage estimates from models with different horizontal resolutions and found that at lower resolutions

Agulhas leakage is overestimated by about a third, thus emphasizing the importance of resolving finer-scale dynamics. The relatively large range of Agulhas leakage estimates could be related to the high variability of interocean exchanges that was identified by *Reason et al.* [2003] and the fact that large leakage estimates depend on the presence of an Agulhas ring that tends to be somewhat intermittent; from satellite sea surface height data, *Schouten et al.* [2000] counted about five rings per year that were irregularly spawned between November 1992 and December 1996. Eulerian estimates of Agulhas leakage have the difficulty of separating the contributions from Indian Ocean Central Water (IOCW) and South Atlantic Central Water (SACW) due to their similar water mass characteristics. Although there is no general consensus of the exact contribution of the Agulhas to the Benguela Current, *Garzoli and Gordon* [1996] found that a correlation exists between the strength of the Benguela Current and the salinity of the thermocline layers, suggesting that variations in the transport of the Benguela Current are indeed related to the relatively saline Agulhas input.

The Benguela Current can thus be thought of as the vehicle for passage of Agulhas Rings and eddies into the Atlantic Ocean and while there is no consensus on the exact volume of water of Indian Ocean origin within the Benguela Current, the fact that it introduces an enormous pool of energy is unequivocal. For example, *Matano and Beier* [2003] found that the eddy fluxes of the Agulhas eddies supply most of the energy of the Benguela Current and the southeastern portion of the Cape Basin has been dubbed the "Cape Cauldron" by *Boebel et al.* [2003] due to its highly energetic nature as a result of the interaction of Agulhas Rings, eddies, and filaments as well as mesoscale features associated with the shelf-edge and upwelling front. Cyclone/anticyclone interaction in the Cape Basin results in vigorous mixing at small scales that can impact productivity in the region by introducing extreme vertical velocities that can advect nutrients into or out of the euphotic zone. *Gruber et al.* [2011] have shown that contrary to what has been found for open-ocean regions, mesoscale and submesoscale eddies in coastal upwelling regions tend to reduce biological productivity by transporting nutrients offshore. Using FSLE (Finite Size Lyapunov Exponent) analysis, *Rossi et al.* [2008] quantified the inverse relationship of lateral mixing and chlorophyll in the southern Benguela region as suggested by the work of *Gruber et al.* [2011]. The highly turbulent regime associated with the passage of Agulhas Rings and eddies in the offshore region of the southern Benguela system therefore has the potential to indirectly impact the ecosystem.

More direct impacts of the Agulhas on productivity in the Benguela system are the interactions of Agulhas Rings or leakage with the upwelling regime itself. The upwelling front defines the seaward boundary of the upwelling regime and mesoscale features and interactions associated with it are likely to have crucial implications for cross-shelf exchanges and therefore productivity. South of Lüderitz, which is often considered the boundary between the northern and southern upwelling regimes, the upwelling front is well-defined and tends to follow the shelf-edge, while it is more diffuse in the north [*Shannon and Nelson*, 1996]. The upwelling front is characterized by filaments that extend 100–500 km beyond the upwelling front [*van Fore-est et al.*, 1984], but single filaments have been observed to extend considerable distances offshore (about 1000 km) and are usually confined to the vicinity of Lüderitz [*Lutjeharms et al.*, 1991]. The largest filaments develop meanders of the order of 250 km in wavelength and 100 km in amplitude. According to *Lutjeharms et al.* [1991] and *Duncombe-Rae et al.* [1992], the meandering nature of the filaments implies the interaction between filaments at the front and the passage of Agulhas Rings. The significance of upwelling filaments is in their ability to advect upwelled water, rich in nutrients and biota, offshore. Large and persistent filaments can therefore have severe ramifications for the productivity of the upwelling ecosystem. A filament investigated by *Duncombe-Rae et al.* [1992] extended some 450 km offshore and had become entrained in an Agulhas ring and could have resulted in an offshore volume transport of 1.5 Sv.

Lutjeharms and Stockton [1987] observed a large number of cyclonic eddies within the upwelling system and noted that they were preferentially situated downstream and offshore of the major upwelling cells and that they did not have a seasonal signal. Satellite images investigated by *Strub et al.* [1998] revealed their formation within the cool upwelling regime, followed by their offshore advection. The formation of these eddies is abundant off the Cape Peninsula and one such feature was studied by *Lutjeharms and Mathyssen* [1995] who found that they are not correlated with variations in the wind. *Lutjeharms and Stockton* [1987] suggested that filaments originating at the Agulhas retroflection could have a role to play in their initiation. A more recent study by *Rubio et al.* [2009] of satellite and model data showed that the cyclonic eddies are generated along the frontal region and have life spans of several months with typical diameters of about

60 km in deeper regions of the continental slope (deeper than 2500 m) and about 20 km in the shallower regions (500–2500 m). They are shown to be recurrent throughout the year and drift westward with volumes of 2–4.5 $\times$ 10^{12} m^3, which is significant in terms of cross-shelf exchanges.

A dominant feature of shelf-circulation in the southern Benguela region is the Goodhope Jet, which was anticipated (based on intense horizontal density gradients) and then observed and described by *Bang and Andrews* [1974]. The jet is located over the steep shelf in this region and has been observed to be permanently present irrespective of wind conditions [*Nelson and Hutchings*, 1983]. The jet has characteristic speeds of 50 cm s^{-1} and a width of 20–30 km. From satellite altimetry, *Strub et al.* [1998] noted a seasonal strengthening of the jet, which they associated with the injection of water with high steric heights, via Agulhas Current influx, on the offshore side of the jet and adjacent to the cold upwelled waters at the coast. It has been described by *Shannon and Nelson* [1996] as a convergent NW-oriented current system on the western Agulhas Bank that funnels into the west coast and bifurcates at Cape Columbine into an offshore and alongshore component. The importance of the jet lies in the fact that it transports fish eggs and larvae from their spawning ground on the Agulhas Bank to their nursery area in St. Helena Bay [*Shelton and Hutchings*, 1982].

The role of the Agulhas in the Benguela system via eddy fluxes, leakage, and the direct interaction of rings and filaments is frequently suggested, but aside from measurements of its transport contribution to the Benguela Current, it is less often explicitly investigated with regard to its impact. While it is clear that the Agulhas has an enormous signal in the Benguela system, it is difficult to quantify its impact on local dynamics. In the work of *Treguier et al.* [2003] it was shown that the dominance of anticyclonic rings over cyclonic eddies does not allow for the transient component of flow to be entirely removed from the mean state. In addition, *Matano and Beier* [2003] have shown that most of the energy of the Benguela Current is supplied by eddy fluxes. In order to obtain more information on the role of the Agulhas in Benguela Current dynamics, we investigate a model experiment in which the direct impact of the Agulhas Current has been removed.

2. Methods

The modeling strategy of this work involves running two identical numerical simulations of the hydrodynamic regime of the Benguela system, one of which is not subject to the direct influence of the Agulhas Current. REF and NOA are used to denote the reference simulation and no Agulhas experiment, respectively.

2.1. ROMS

The Regional Ocean Modeling System (ROMS) is a split-explicit, free-surface, topography-following vertical coordinate model that is well suited for regional applications [*Shchepetkin and McWilliams*, 2005, 2008]. It solves the incompressible primitive equations based on the Boussinesq and hydrostatic approximations and is coupled to advection-diffusion schemes for potential temperature and salinity as well as a nonlinear equation of state for density. The advection scheme is third-order upstream biased, which reduces dispersion errors, essentially enhancing precision for a given grid resolution [*Shchepetkin and McWilliams*, 1998]. The implementation of a higher-order advection-diffusion scheme has led to the development of spurious diapycnal mixing in sigma-coordinate models. A solution to this problem was addressed by *Marchesiello et al.* [2009] and involves the splitting of advection and diffusion, the latter of which appears as a biharmonic operator. This solution was implemented in our configuration in order to preserve the low diffusion and dispersion benefits of the original scheme while maintaining water mass characteristics. Explicit lateral viscosity is everywhere zero except in sponge layers at open boundaries, where it increases smoothly toward the edge of the domain. Open boundary conditions of the parent domain are a combination of outward radiation and nudging toward prescribed external boundary conditions and are described by *Marchesiello et al.* [2001]. Subgrid-scale vertical mixing is introduced by the nonlocal K-profile parameterization (KPP) scheme [*Large et al.*, 1994]. The bottom friction coefficient is calculated through the use of a logarithmic boundary layer formulation with a bottom roughness of 10 cm.

2.2. Model Configuration

In order to maximize computing efficiency, the Adaptive Grid Refinement in Fortran (AGRIF) nesting capability [*Debreu et al.*, 2008] of ROMS was employed. The nested approach has been evaluated by *Penven et al.* [2006a] and is designed such that the boundary conditions of a high-resolution "child" domain are provided by a lower-resolution "parent" domain within which the child is embedded. This allows for more consistent and better resolved boundary conditions for the child than can be obtained from in situ measurements or from low-resolution global models, respectively. Our simulations make use of the two-way nesting approach, which also allows the child solution to update the parent solution [*Debreu et al.*, 2012]. A major advantage of the two-way nesting approach is that the parent-child feedback allows for a more accurate passage of features from the child to the parent than in the one-way nesting approach. The two-way nesting approach is therefore particularly beneficial for a child domain that includes the highly turbulent Cape Basin region, which is subject to the passage of large-scale (200–300 km in diameter) Agulhas Rings. The topography of the nested configuration is a bilinear interpolation of the 1′ General Bathymetric Chart of the Oceans (GEBCO; available online at http://www.gebco.net). In order to further avoid the problem of pressure gradient errors, the bathymetry is smoothed in order to maintain a slope parameter of less than 0.2 (for a description of the method, refer to *Penven et al.* [2007]). The parent and child bathymetries are smoothly connected with a relation that uses an alpha parameter that is 1 (i.e., the bathymetry is coarse and is consistent with the low-resolution parent domain) at the parent-child boundary and 0 (i.e., the bathymetry is totally refined to the grid of the child) at 15 grid cells from the boundary. Both the parent and child domains have 32 topography-following vertical levels that are stretched toward the surface, with a theta_s parameter of 6 [*Haidvogel and Beckmann*, 1999]. Because of the experimental approach of this study, the model configuration was kept relatively simple by running it in climatological mode. A 0.5° QuikSCAT climatology, based on data spanning 2000–2007, was used for the wind forcing and surface heat and salt fluxes were obtained from the Comprehensive Ocean-Atmosphere Data Set (COADS) climatologies [*Da Silva et al.*, 1994]. Initialization was from a state of no-flow and mean January temperatures and salinities from the World Ocean Atlas 2005 (WOA) [*Conkright et al.*, 2002]. ROMS addresses the lack of an atmosphere-ocean feedback term by the parameterization of a linearized atmosphere-ocean feedback term for the surface heat flux. This SST "restoring" is done using the 9 km Pathfinder climatological SST product and a similar surface salinity correction scheme is applied using the COADS climatological data due to the paucity of evaporation-precipitation forcing data. The nested configuration is run for 10 years, of which the first two are considered the spin-up period after which the model solution reaches statistical equilibrium when a robust seasonal signal approximately repeats itself and no temporal drift is evident (in energy, temperature, or salinity). Analyses for this paper are based on model output spanning years 3–10. The parent domain is known as the Southern African Experiment (SAfE) and was designed by *Penven et al.* [2006b] to capture salient southern African oceanographic features. The domain encompasses the region spanning 2.5°W–54.75°E and 46.75°S–4.8°S and has a horizontal resolution that ranges from 19 km in the south to 27.6 km in the north, allowing for the resolution of Agulhas Rings, which have a length scale of about 300 km [*Penven et al.*, 2006b]. The boundary conditions for the parent domain are supplied by WOA 2005 [*Da Silva et al.*, 1994] temperatures and salinities from which geostrophic velocities are calculated, together with the QuickSCAT climatological wind stresses for Ekman transports. The child domain encompasses the greater Benguela system, inclusive of both the nearshore upwelling regime as well as the large-scale offshore current domain, spanning 3.9°E–19.8°E and 35.6°S–12.1°S and has a horizontal resolution that ranges from 9 km in the north to 7.5 km in the south. Given that the first baroclinic Rossby radius within the child domain ranges from ∼30 km in the south to ∼70 km in the north [*Chelton et al.*, 1998], the child domain captures the mesoscale variability in the region, in agreement with *Soufflet et al.* [2016]. The parent-child configuration described above has been thoroughly evaluated with respect to the equilibrium dynamics of the Benguela system in *Veitch et al.* [2009, 2010].

2.2.1. Removing the Agulhas

The model experiment in which the direct effect of the Agulhas is removed from the Benguela is based on the same ROMS model configuration described in the previous section, except that the Agulhas Current is diverted eastward before reaching the tip of Africa. This method takes advantage of the natural tendency of the Agulhas Current to retroflect earlier than its usual location [*van Aken et al.*, 2013] and is done by adapting the land mask so that a curved dam extends off the east coast of South Africa at 30°S to about 36°E [*Chang*, 2009]. As an indication of the effect on the mean surface geostrophic flow by the diversion of
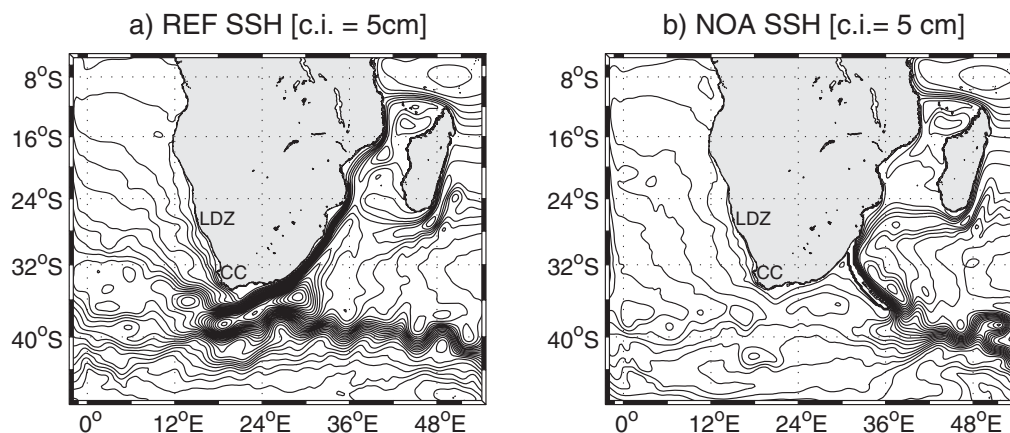
Figure 1. Lines of constant sea surface height for the REF (a) and NOA (b) simulations, representative of surface geostrophic flow. LDZ is Lüderitz and CC is Cape Columbine. The contour interval is 5 cm.

the Agulhas Current in the NOA experiment, Figure 1 shows the annual mean sea surface height for both the NOA and REF simulations. The retroflection of the Agulhas Current eastward before it reaches the tip of Africa prevents rings and eddies shed at its retroflection from entering the Benguela system. Since it exaggerates a natural tendency of the Agulhas Current to retroflect early, the NOA model solution is still stable and physically meaningful. Nevertheless, the change in the mean state, surface manifestation of the Benguela Current is significant: the intense, meandering flow punctuated by cyclonic/anticyclonic features becomes a weaker, more uniform north-westward flow.

3. Results

3.1. Thermohaline Characteristics

As a first approach at investigating the role of the Agulhas on the mean state of the Benguela Current system, Figure 2 shows the differences between the REF and NOA mean SSTs and seasonal standard deviations (STD). SSTs are up to 3.5°C higher in the REF simulation with greatest differences occurring offshore of the shelf-edge and decreasing toward the north. The difference in SST increases rapidly at the shelf-edge, suggesting that the Agulhas has limited influence on the SSTs on the shelf and also that it has a significant role to play in density-driven shelf-edge jets. The shelf area in the southern Benguela tends to be slightly warmer (0–0.5°C) in the REF simulation, with two exceptions where the water is slightly (<0.5°C) cooler: a plume along the coast that broadens northward from about 32°S to just south of Lüderitz and two small tongues within St Helena Bay. These along-shelf variations in the SST difference between models imply the Agulhas's role in upwelling front dynamics and cross-shelf exchanges in the southern Benguela.

The seasonal standard deviations of SST shown in Figures 2d and 2e reveal a stronger seasonal signal in the southern Benguela, particularly in the offshore region, in the NOA experiment. This finding is consistent with the high level of mesoscale variability (and therefore high mixing and diffusion) that is observed in the Cape Basin region as a result of Agulhas leakage in the form of rings, eddies, and filaments, which inject warm water into the region throughout the year. In both the REF and NOA simulations, the seasonal standard deviation increases offshore due to the "masking" of nearshore variability by the strong seasonal upwelling signal that brings cold water to the surface during summer, thus opposing the seasonal warming and cooling.

The manifestation of the upwelling front in terms of SST provides an indication of nearshore-offshore interaction processes. Figure 3 is 2 day averaged "snapshot" of SSTs derived from the REF and NOA simulations during the summer season and provides a clear impression of the impact that the Agulhas has on the upwelling front, particularly in the southern Benguela region. In the REF experiment we see an upwelling regime that is more constrained to the shelf-region and that is marked by a sharp front that tends to remain inshore of the shelf-edge. This distinct dichotomy between the warm offshore and cool nearshore waters as
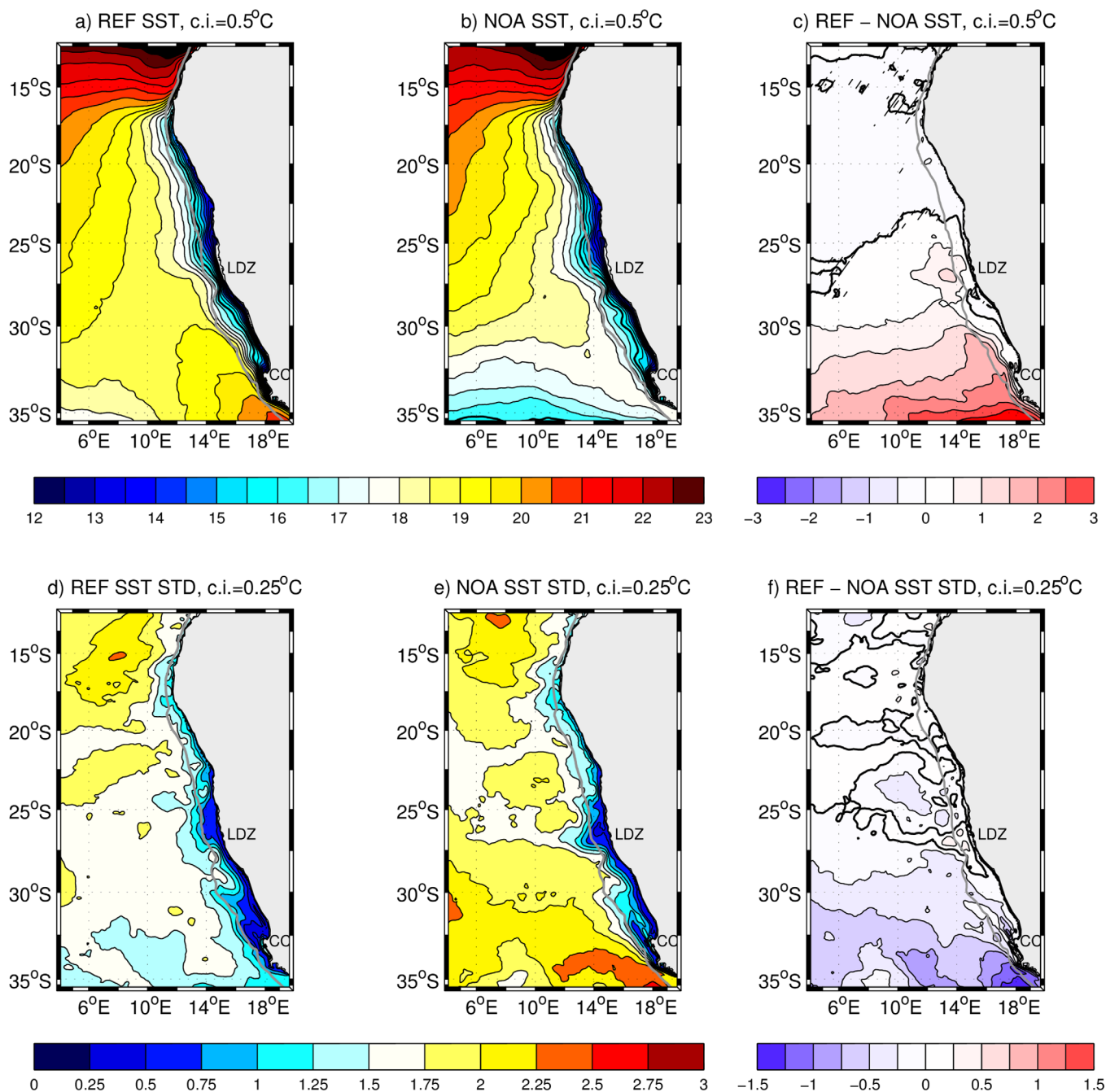
Figure 2. (a, b) Annual mean sea surface temperature (SST), (d, e) seasonal standard deviations, and (c, f) the differences between the REF and NOA runs for each. The cross-hatched regions of Figure 2c show where the differences are insignificant. The 500 m isobath is shown as a gray line. LDZ is Lüderitz and CC is Cape Columbine.

well as associated jet currents exists from as far south as Cape Agulhas to at least 30°S. On the other hand, without the influence of the Agulhas, the upwelling front in the southern Benguela extends further offshore northward of Cape Columbine and is more diffuse, being characterized by short filaments extending offshore. South of Cape Columbine, where the shelf is narrower, the upwelling front is as intense as in the REF simulation. In both the REF and NOA simulations, large offshore filaments are present in the vicinity of Lüderitz, which suggests that they are generated locally by the intense, perennial upwelling-favorable wind there in combination with the offshore geostrophic flow, which is dependent on the large-scale wind stress curl, and that they do not rely on features associated with Agulhas influx [*Veitch et al.*, 2010].
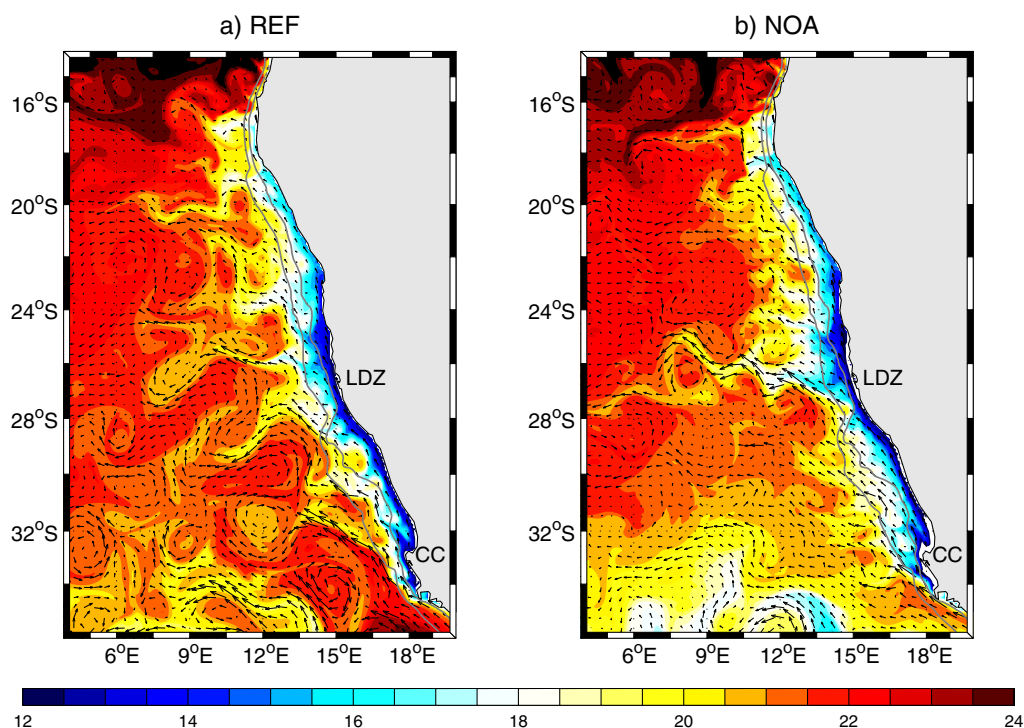
Figure 3. "Snapshot" of SST (units: °C) and surface current vectors from model year 8, month 2 for the REF and NOA simulations (right and left, respectively). The gray lines are the 200 and 500 m isobaths. LDZ is Lüderitz and CC is Cape Columbine.

The mean position and intraseasonal variability of the summer upwelling front confirms the persistence of the features described above. After several attempts at formulating the best method of extracting the location of the upwelling front, the most accurate and consistent proved to be the simplest. At each latitude the location of the main upwelling front is identified as follows:

$$T_{front} = 0.25T_{coast} + 0.75T_{offshore}, \tag{1}$$

where T_{front} is the temperature representative of the upwelling front, T_{coast} is the average SST between the coast and the location of the 80 m isobath and $T_{offshore}$ is the average offshore SST, averaged between 500 and 1000 km. While the model contains a surface SST restoring term (based on Pathfinder SSTs for both the REF and NOA simulations) in order to take into account the air-sea exchange feedback term, its effect contributes less than 15% to the total surface heat flux of the child domain, and therefore should not significantly influence our study.

Based on this method, the location of the summer mean upwelling front for the NOA and REF simulations is shown as a green line in Figure 4 while the black dots show the locations of the upwelling front, based on each two-daily averaged summer SST (for clarity, only one out of twenty alongshore positions are shown per two-daily average) and reveals the intraseasonal variability resolved by the climatologically forced simulation. In both simulations the mean upwelling front extends further offshore in the northern Benguela where the shelf is narrower (see dashed red line) than in the southern Benguela and is consistent with that resolved by satellite data in *Lutjeharms and Stockton* [1987]. The coherence between the location of the upwelling front and the shelf-edge is particularly distinct in the REF simulation: the seaward standard deviation line (yellow) follows the shelf-edge until 30°S, while in the NOA experiment it lies beyond the shelf-edge (consistent with the filaments in Figure 3) and the mean position of the upwelling front (in green) follows it only until about Cape Columbine (at 33°S). Southward of Cape Columbine, where the shelf is narrow, in both simulations the upwelling front never extends far offshore suggesting an intense front and associated jet in both which can be seen in the vectors in Figure 3.

Maximum offshore excursions of the front in both simulations correspond with the location of the most vigorous and perennial upwelling cell in the Benguela system, Lüderitz, a distinct offshore surface geostrophic
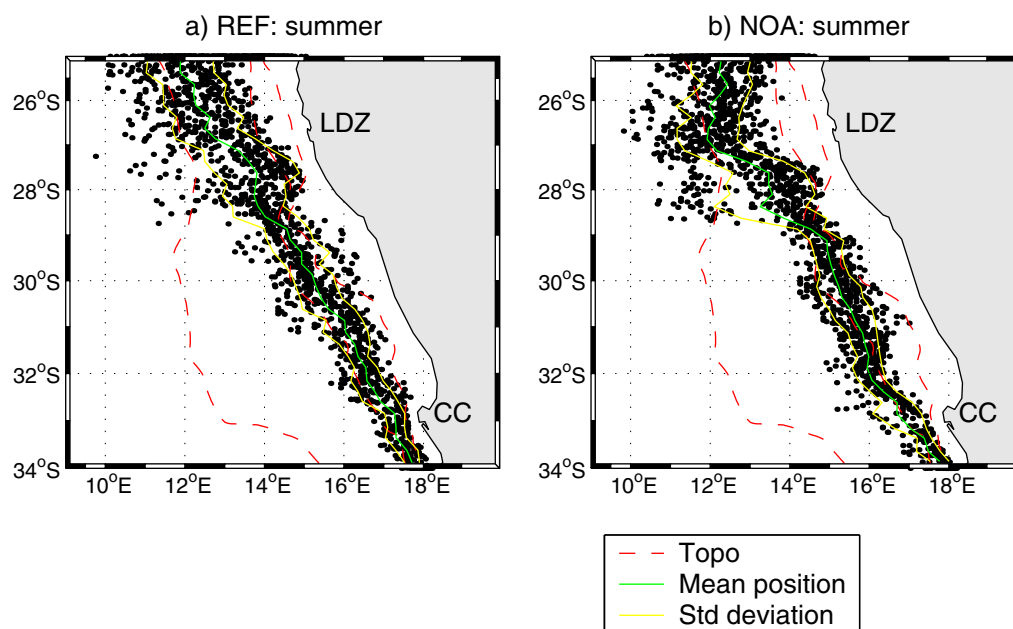
Figure 4. Summer front statistics for the REF and NOA simulations (left and right, respectively). Red lines represent the 200, 500, and 4000 m isobaths, the green line is the mean summer position of the front, the yellow lines show the standard deviation and black dots show the two-daily locations of the front. LDZ is Lüderitz and CC is Cape Columbine.

flow (see the streamlines in Figure 2), high surface EKEs (see Figure 8) and a sudden narrowing of the shelf. The maximum offshore extent of the upwelling front at Lüderitz for both is of the order of 600–700 km.

Figure 5 shows the alongshore averaged temperature and salinity sections for both simulations and their differences in a representative section of the southern Benguela and give a better idea of the impact of Agulhas influx on the water mass properties. Other than over the shelf, deepening from the surface at the coast to about 100 m in the vicinity of the shelf-edge and at depths greater than 800 m, water in the southern Benguela is everywhere cooler in the NOA experiment. The warmer water in the NOA simulation over the shelf appears to be related to an upward tilt of the isotherms in the REF simulation in this region as a result of dynamic uplift as the warmer waters associated with Agulhas influx move past the shelf-edge. The salinity sections show that Antarctic Intermediate Water (AAIW), characterized by a salinity minimum, exists deeper in the REF simulation than in the NOA simulation due to mixing with higher-salinity water of Indian Ocean origin in the REF simulation. At depths of greater than about 100 m the NOA simulation has lower salinities than the REF simulation, with the greatest differences occurring in the vicinity of the central water mass (200–500 m). It is noteworthy and somewhat unexpected that in the upper 100 m the NOA simulation has higher salinities than the REF simulation. This could be partly due to the more extreme dynamic uplift in the REF simulation that brings fresher and colder water onto the shelf than in the NOA experiment. However, the lower-salinity signal in the REF simulation extends further offshore than the lower-temperature signal. The extended region of lower salinity in the REF simulation may be the result of the intense mesoscale variability associated with Agulhas influx in the REF simulation providing the means for mixing with the fresher upwelled surface waters, while the lower-temperature signal does not extend as far offshore due to surface heating.

The temperature-salinity (T-S) plots shown in Figure 6 provide a succinct summary of the thermohaline impact of the Agulhas on the southern Benguela system. Three profiles for both the REF and NOA simulations are shown, representative of the shelf (100 km offshore), shelf-edge (200 km offshore), and offshore (500 km offshore) regions. The surface waters of the NOA experiment are more saline than the REF simulation, except for the upper 10 m on the shelf, which is a result of the offshore advection of fresher upwelled water. Surface waters, as defined as the top "tail" in the T-S plots, are deeper in the REF simulation than in the NOA experiment, particularly at the shelf-edge and offshore of it, by about 100 m. The surface water of the REF simulation is separated into two distinct masses: the fresher and warmer upper 10 m is likely to
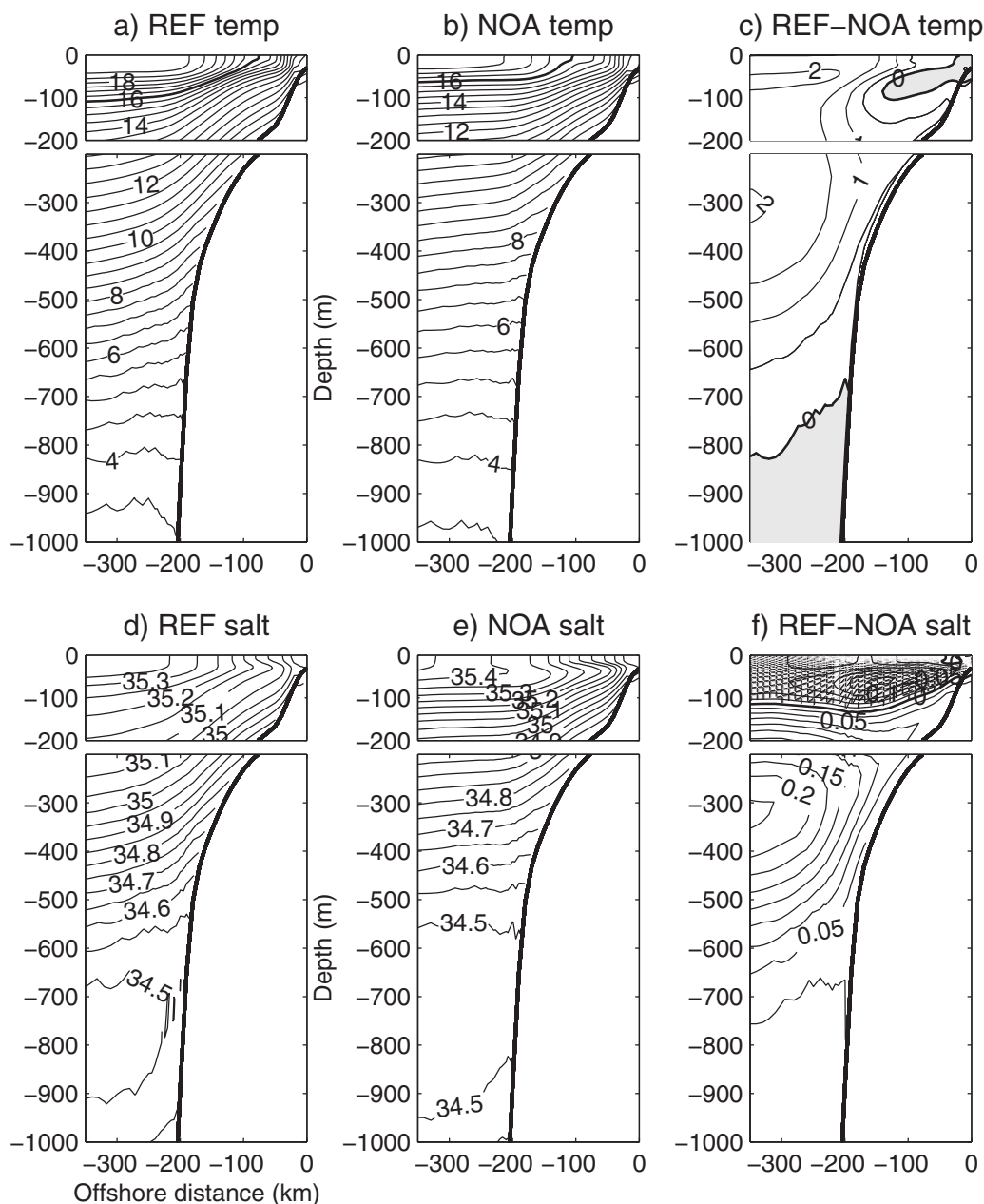
Figure 5. Annual mean temperature (top) and salinity (bottom) sections in the southern Benguela for the REF and NOA simulations and their difference (which is significant throughout the section at the 95% level).

originate from coastal upwelled waters, while the deeper surface waters may be associated with the shelf-edge, dynamic uplift as previously discussed. In all profiles, more so in the offshore profiles, the central water mass is fresher in the NOA experiment. At depths of greater than about 1000 m the water mass characteristics of the two simulations start to converge.

3.2. Large-Scale Transport
The contribution of the Agulhas to the Benguela Current transport values is known to be significant and is suggested in the surface geostrophic current patterns revealed by the lines of constant SSH for the REF and NOA simulations shown in Figure 1. Figure 7 shows the alongshore averaged transport (integrated to a depth of 1000 m) in the southern Benguela from both the REF and NOA simulations as well as the transport derived from a Sverdrup relation, assuming an active layer of 1000 m [*Veitch et al.*, 2010]. The two distinct
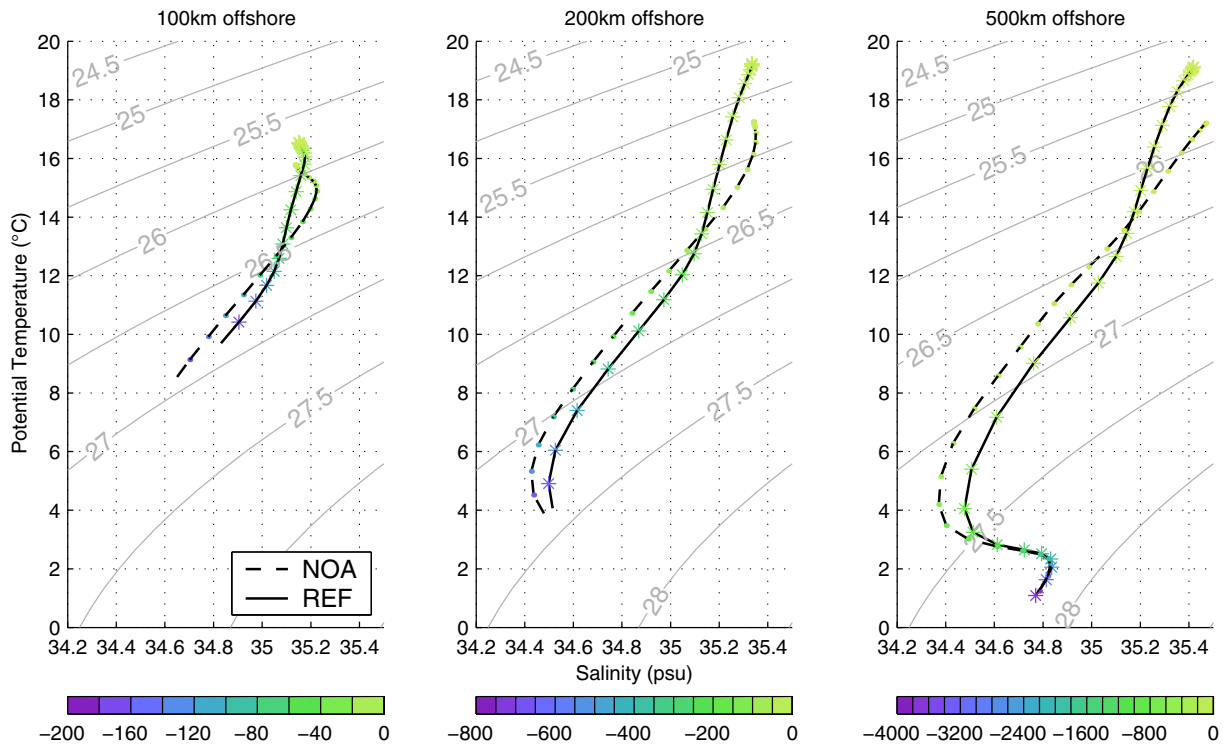
Figure 6. T-S plot for the southern Benguela for the REF and NOA simulations with characteristic water mass properties for South Atlantic, Tropical Atlantic, and Agulhas waters shown in color.
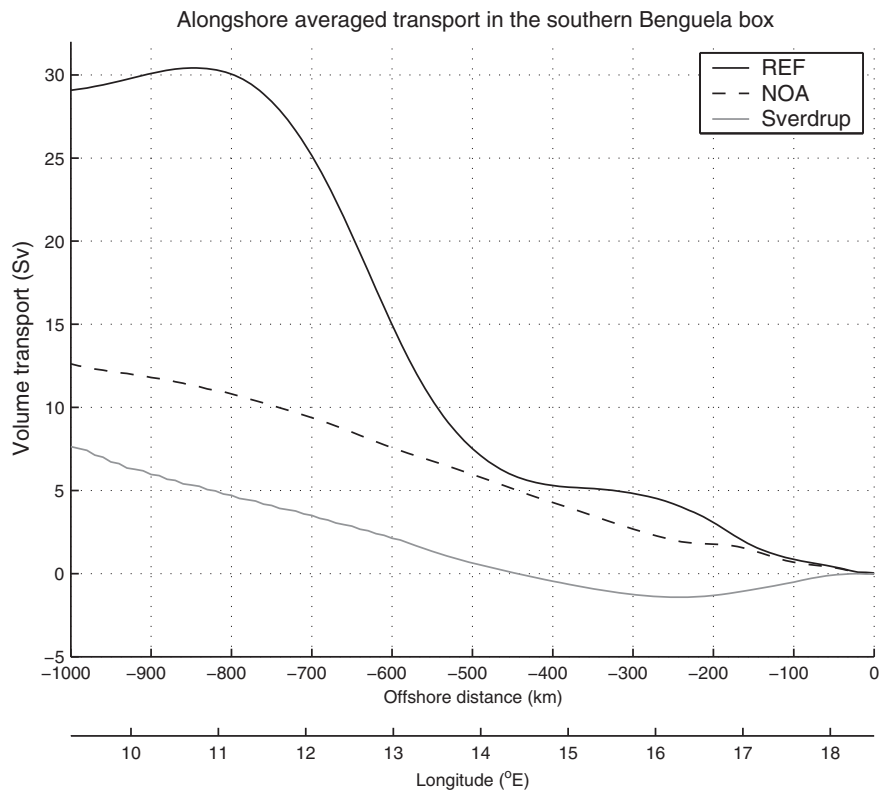

Figure 7. Transport, integrated between 0 and 1000 m, across 30°S for the REF and NOA simulations as well as derived from the Sverdrup relation.
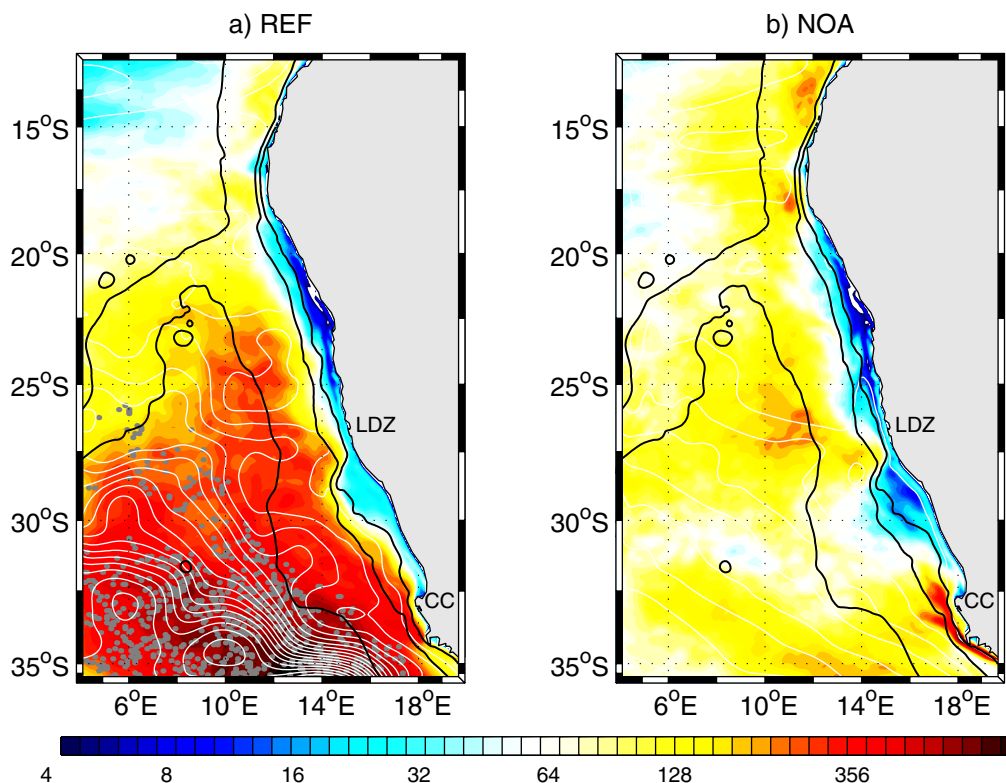
Figure 8. Surface eddy kinetic energy (EKE, units in cm^2 s^{-2}) for the REF (left) and NOA (right) simulations with 0–1000 m, depth-integrated streamlines of flow (interval: 2 Sv) shown in white and the 200, 500, and 4000 m isobaths shown in black. Gray dots represent the tracks of Agulhas Rings in the REF simulation. LDZ is Lüderitz and CC is Cape Columbine.

"streams" of equatorward transport are evident in the REF simulation, one is the previously investigated shelf-edge jet, which is approximately 200 km offshore and has a transport of about 5 Sv, and the other is the mean manifestation of the Benguela Current, which has a transport of about 25 Sv and peaks some 800 km offshore. The equatorward transports in the NOA experiment do not exhibit two distinct currents. Instead, the weaker equatorward current over the shelf (roughly 200 km from the coast) has a transport of no more than 1 Sv, while the equatorward flow from the shelf-edge to 1000 km offshore has a transport of about 10 Sv. This suggests that in our model the Agulhas contributes about 15 Sv to the transport of the Benguela Current, which is the same as the Agulhas leakage estimate given in *Richardson* [2007]. Although shifted by about 5 Sv due to shelf processes, the equatorward transport follows a line parallel to the Sverdrup transport (the thin line in 7) offshore of 350 km from the coast, thus confirming that the large-scale flow regime in the NOA experiment is consistent with Sverdrup dynamics. Closer inshore, the Sverdrup relation predicts the existence of a net poleward flow associated with cyclonic wind stress curl between about 100 and 400 km offshore; however, it does not appear in the depth-integrated transport plot for the REF and NOA simulations due to the more intense and shallower equatorward transports in each that are driven by dynamic upwelling and intense upwelling fronts associated with the Cape Columbine upwelling plume, respectively.

The surface eddy kinetic energy (EKE) for the REF and NOA simulations are shown together with transport (integrated from the surface to 1000 m depth) plots in Figure 8 in order to reveal the intense variability associated with the mean manifestation of the Benguela Current and how it differs between the two simulations. Black lines (the 200, 500, and 4000 m isobaths) indicate the approximate position of the shelf-edge and the steepness of its slope as well as the position of the Walvis Ridge. Note that a log-scale is used for the color bar in order to sufficiently capture the relatively low EKE near the coast as well as the very high EKE offshore. The gray dots represent the tracks of anticyclonic eddies identified in the REF model output for model years 3–6. The eddy-tracking tool makes use of the Okuba-Weiss parameter and was developed by *Penven et al.* [2005]. By removing Agulhas influx, the extremely high offshore mesoscale variability

characteristic of the southern Benguela disappears. The most intense mean flow in the REF simulation is a meandering flow in the offshore region that is superimposed on highest EKEs and is in the corridor of Agulhas Rings. This suggests that the intense mean Benguela Current is partly a manifestation of the passage of large-scale Agulhas Rings. While the REF simulation has a significantly stronger mean flow than the NOA experiment, both simulations exhibit peak EKEs in regions of most intense flow (represented by the most closely spaced isolines): the intense shelf and shelf-edge jet feature in the NOA and REF simulations, respectively, and the offshore stream of the Benguela Current in both simulations. In the REF simulation the high EKEs associated with the mean manifestation of the Benguela Current are by far the most intense in the domain. Removing the Agulhas shows the distinct offshore transport separating the northern and southern Benguela systems (25°S–28°S) is a source of locally generated mesoscale variability and is likely a result of the propensity for large upwelling filaments in this region [*Lutjeharms et al.*, 1991; *Shillington et al.*, 1990]. The overlay of the position of the Walvis Ridge on the surface EKEs shows that mesoscale variability associated with Agulhas leakage does not extend northward beyond it, illustrating a potential role of this topographic barrier.

3.3. Currents on the Shelf and Slope

Annual mean horizontal and vertical currents at the coast, over the shelf and within a few hundred kilometers of the shelf-edge for the REF and NOA simulations, shown in Figure 9, provide a clear indication of the dynamic differences that relate to the disparate thermohaline characteristics already mentioned. In the REF simulation two very distinct alongshore jets are evident, one within 50 km of the coast that forms part of the coastal upwelling system of currents (i.e., a clear "cell" of upward velocity and an offshore and compensatory onshore flow beneath it). The other jet is present over the shelf-edge and is tied to upward velocities that are present from a depth of about 10 m to the approximate depth of the shelf-edge and are of the order of the upwelling velocities at the coast. While the coastal upwelling system of currents is present in much the same combination and intensity in the NOA experiment, the shelf-edge feature is present but an order of magnitude weaker than in the REF simulation and the intensified alongshore current exists over the shelf, rather than at the shelf-edge. Terms of the momentum balance equations confirm that, away from the surface and coastal boundaries, these equatorward jets in both simulations are geostrophic. The shelf-edge upwelling feature, particularly intense in the REF simulation, can therefore be explained by the necessary uplift of isopycnals (seen as an uplift of isotherms in Figure 5) in order to maintain the intense zonal pressure gradient required by the fast shelf-edge jet. On the other hand and given that the average alongshore sections of currents, temperature, and salinity are taken just north of Cape Columbine, the shallow alongshore current over the shelf particularly evident in the NOA experiment and perhaps masked by the intense shelf-edge jet feature in the REF simulation could be related to the northward advection of the Cape Columbine upwelling plume that can be seen both in the mean state SSTs (Figure 2) as well as in a snapshot of SSTs (Figure 3). The poleward undercurrent, forced by the cyclonic wind stress curl [see *Veitch et al.*, 2009, Figure 2], is present in both simulations and is associated with downward velocity in order to conserve potential vorticity.

3.3.1. The Good Hope Jet

Shelf-edge jets, associated with an upward displacement of isopycnals [*Shannon and Nelson*, 1996], are relatively persistent in the southern Benguela. We focus here on the Good Hope Jet that exists southwest of Cape Town, extending northwestward from the western Agulhas Bank [*Shannon and Nelson*, 1996] and has been identified as a key factor in transporting fish eggs and larvae from their spawning ground on the Agulhas Bank to their nursery area in St Helena Bay and in the high productivity of the southern Benguela region [*Shelton and Hutchings*, 1982]. The intense horizontal gradients observed by *Bang and Andrews* [1974] was the first evidence for its existence, and *Strub et al.* [1998] used satellite altimetry to investigate the seasonal signal of its surface manifestation. They noted a seasonal intensification that they associated with the interplay of the injection of high steric heights via Agulhas influx and the low steric heights associated with the coastal upwelling regime. However, work carried out by *Nelson* [1985] during a slackening phase of the upwelling favorable wind suggested the permanence of the jet. The results of the NOA experiment allow us to reinforce current theories about the role of Agulhas influx on the jet in a more conclusive manner.

Figure 10 presents the summer and winter mean current field at the surface for both the NOA and REF simulations and shows that in both cases an intense equatorward jet exists over the shelf-edge region (approximately between the 200 and 500 m isobaths) off Cape Point. During summer months, the jet is far more
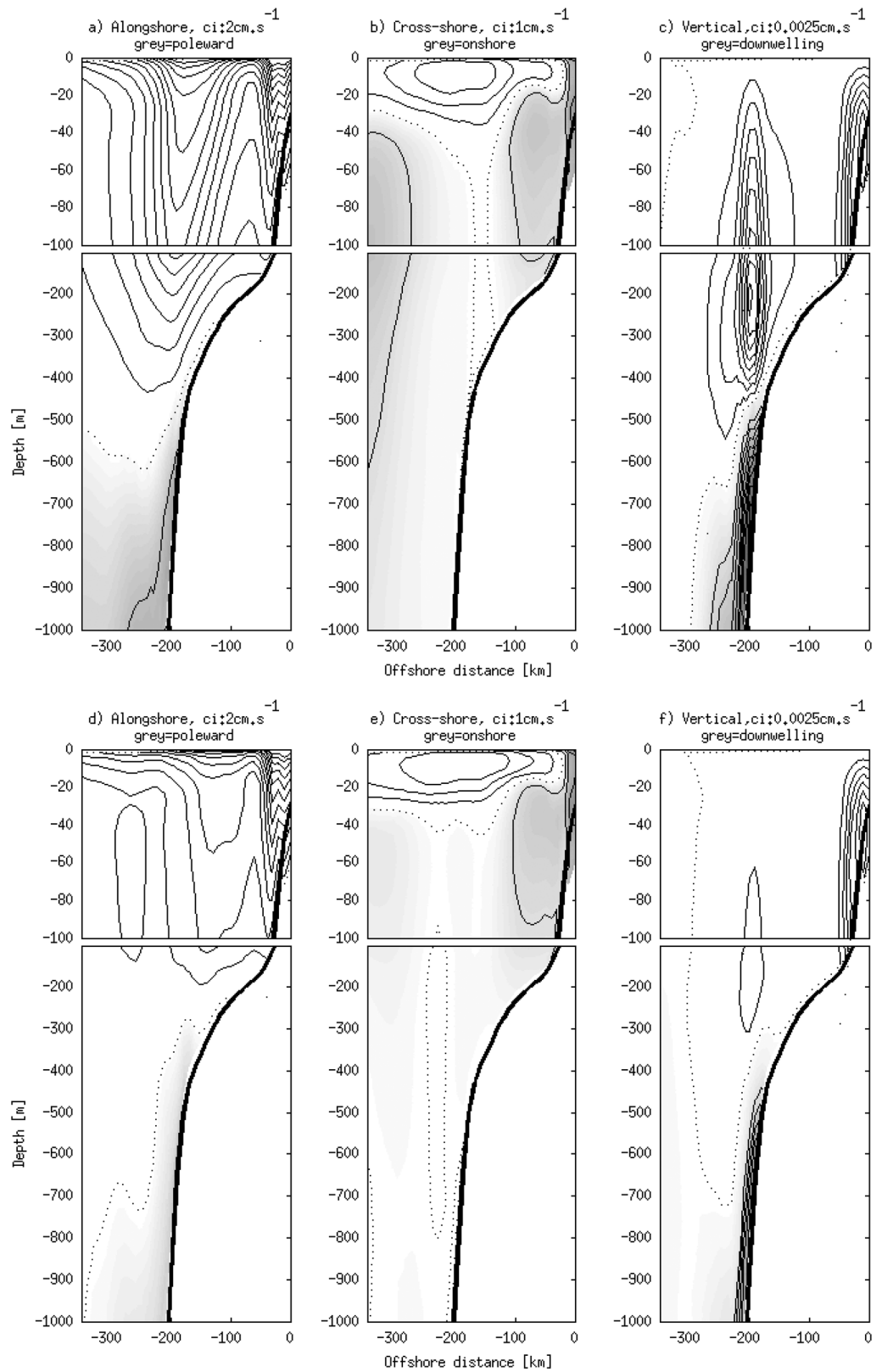
Figure 9. Annual mean alongshore, cross-shore, and vertical velocities in the southern Benguela for the REF and NOA simulations.
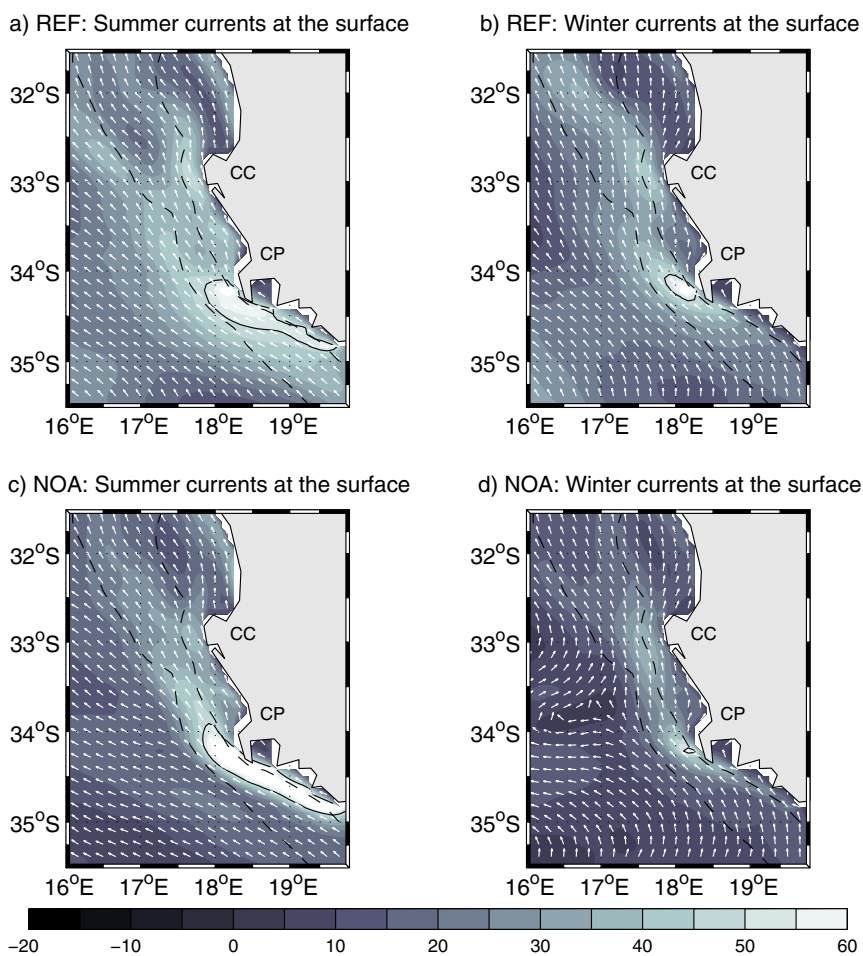
Figure 10. Winter and summer (left and right, respectively) mean currents in the southern Benguela for the REF and NOA simulations (bottom and top, respectively). The dashed black lines are the 200 and 500 m isobaths, representative of the shelf-edge and the solid black contour is the 50 cm s^{-1} isotach.

intense and extensive, expanding as a continuous jet from Cape Agulhas, with speeds of greater than 50 cm s^{-1}. The summer jet is a more coherent feature in the NOA experiment, distinct from the much weaker currents that surround it, while in the REF simulation fast equatorward velocities persist beyond the shelf-edge. An explanation for the somewhat more intense and confined NOA jet could be the decay of intense horizontal density gradients in the REF simulation associated with the high turbulence of Agulhas influx. In contrast, the fact that fast currents exist beyond the shelf-edge in the REF simulation and not the NOA experiment is likely due to the injection of warm waters of high steric height in the offshore region in the REF simulation. The winter jet in both simulations is very much reduced in extent, particularly in the case of the NOA experiment, with velocities of greater than 50 cm s^{-1} being limited to a small region just offshore of the 200 m isobath, west of Cape Point. Northward of Cape Point, the jet appears to bifurcate into two branches: eastward into Table Bay and northward, continuing along the shelf-edge. The eastward bifurcation into Table Bay appears to be more intense during winter months for both simulations. Further north, a slightly weaker winter and summer jet exists over the 200 m isobath off Cape Columbine, with very little variation in intensity between seasons.

The intense summer jet off the Cape Peninsula can be somewhat explained by the seasonal cycle of upwelling in this region (i.e., enhanced upwelling during summer results in intensified offshore density gradients and in turn increased equatorward flow) for both the REF and NOA simulations. However, the polarity between the intense summer and weak winter jet is amplified in the NOA experiment due to the lack of the constant source of warm water via Agulhas influx. In other words, the warm offshore water from the Agulhas influx intensifies and broadens both the summer and winter jet in the REF simulation. We therefore

hypothesize that the Good Hope Jet is driven by offshore density gradients that are set up by both upwelling dynamics and Agulhas influx, the latter masking the seasonal cycle. While the NOA jet seems then to be primarily forced by upwelling dynamics, it remains present along the 200 m isobath during winter, when the dominant winds are not upwelling favorable.

3.4. Vorticity Budget Analysis

A vertically integrated vorticity balance is used to investigate the relative importance of terms driving the mean flow structure in the upper 1000 m. *Marchesiello et al.* [2003] used the terms of the vorticity balance equation to show that significant departures from the Sverdrup balance occur in the California Current system and are due to the nonlinear terms. Based on the surface EKE plots and the transports in Figure 8, we expect that the nonlinear terms are significant in the southern Benguela system. We examine the terms of the vorticity equation in order to better understand eddy-mean flow interaction processes in the NOA and REF simulations.

A depth-integrated (from the free-surface to 1000 m) vorticity balance equation can be directly derived from the terms of the momentum equation as follows:

$$\int_{-1000}^{\eta} \frac{\partial \zeta}{\partial t} dz = \underbrace{\int_{-1000}^{\eta} f \frac{\partial w}{\partial z} dz - \beta \int_{-1000}^{\eta} v \, dz}_{\nabla \times \text{Coriolis}} \underbrace{- \int_{-1000}^{\eta} \vec{v} \nabla \zeta dz}_{\nabla \times \text{Advection}} \underbrace{+ \nabla \times \frac{\vec{\tau}^{surf}}{\rho_0}}_{\nabla \times \text{Wind stress}}, \tag{2}$$

where ζ is the relative vorticity and η is the free surface. The Coriolis term has been separated into a vortex stretching term (vstretch: $f \frac{\partial w}{\partial z}$, where f is the Coriolis parameter and w is the vertical velocity) and a beta term (beta: βv, where $\beta = \frac{\partial f}{\partial y}$ and v is the meridional velocity component). $\vec{\tau}^{surf}$ is the time mean surface wind stress vector (in N m^{-2}) and ρ_0 is the reference density of sea water. The surface forcing term is the dominant forcing term and far exceeds the interior mixing term, which has therefore been neglected. Since vorticity advection is dominated by the horizontal advection, it can equivalently be written as follows: $\vec{k} \nabla \times [u \frac{\partial u}{\partial x} + v \frac{\partial u}{\partial y}, v \frac{\partial v}{\partial y} + u \frac{\partial v}{\partial x}]$, where u is the zonal velocity component. We separate the total horizontal advection (tadv) into mean and eddy vorticity advection terms, based on a time-mean current. The mean (madv) and eddy (eadv) vorticity advection terms appear as follows:

$$MADV = \int_{-1000}^{\eta} \vec{k} \nabla \times \left[\frac{\partial \bar{u}^2}{\partial x} + \frac{\partial \bar{u}\bar{v}}{\partial y}, \frac{\partial \bar{v}^2}{\partial y} + \frac{\partial \bar{u}\bar{v}}{\partial x} \right] dz, \tag{3}$$

$$EADV = \int_{-1000}^{\eta} \vec{k} \nabla \times \left[\frac{\partial \overline{u'^2}}{\partial x} + \frac{\partial \overline{u'v'}}{\partial y}, \frac{\partial \overline{v'^2}}{\partial y} + \frac{\partial \overline{u'v'}}{\partial x} \right] dz, \tag{4}$$

where $[\bar{u}, \bar{v}]$ and $[u'v']$ are the time-mean and transient, zonal and meridional velocity components, respectively.

Figure 11 shows the alongshore averaged dominant vorticity balance terms integrated from the surface to 1000 m as well as the separation of the total horizontal advection term (TADV) into its mean (MADV) and eddy (EADV) components for both the REF and NOA simulations. Note that the scale of the y axes are different because the vorticity terms are so much smaller in the NOA experiment that in the REF simulation. In the NOA simulation the dominant balance for the large-scale offshore flow is between the wind stress curl and beta effect, with undulating influences from the total advection and vortex stretching terms that are only significant closer to the coast, within the vicinity of the shelf-edge and some 420 km offshore. While the Sverdrup balance dominates the large-scale dynamics, in the region of the shelf-edge at about 220 km offshore, the vortex stretching and total advection terms are dominant and contribute negative and positive vorticity to the vorticity budget, respectively. The total advection term is made up primarily of an eddy advection component with a mean advection term that is not insignificant. These terms are related to the along-shelf advection of cyclonic eddies (consistent with a negative vstretch term) that are generated at the Cape Peninsula and Cape Columbine upwelling cells, a known-feature [*Lutjeharms and Stockton*, 1987] that is present in both the REF simulation and in the NOA experiment. Offshore propagation of features associated with instabilities at the shelf-edge, including cyclonic eddies [*Strub et al.*, 1998], leads to a positive vorticity contribution by the vstretch term via the propagation into deeper water, thus enhancing the
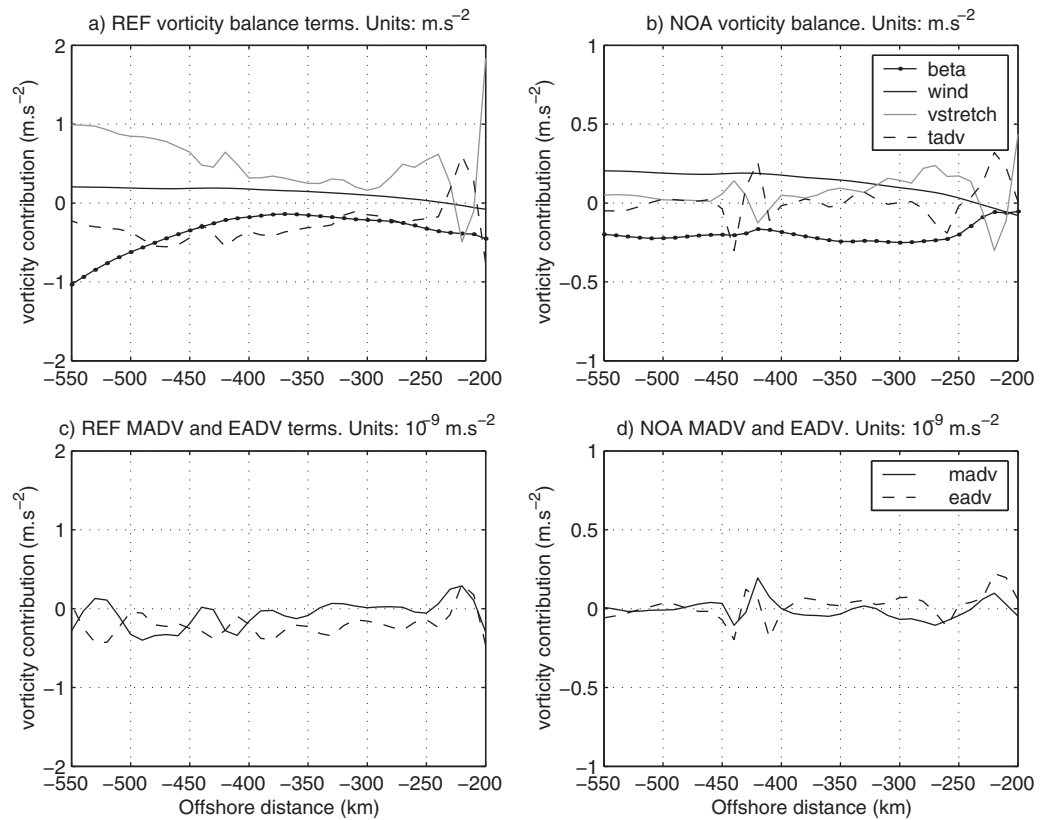
Figure 11. Dominant vorticity balance terms (top) and the advection term separated into its mean and eddy components (bottom) for the REF (left) and NOA (right) simulations. Note the different scales on the y axis.

poleward transport at this location. The significant undulating tadv and vstretch terms between 420–440 km offshore in the NOA alongshore averaged vorticity budget are likely to be related to the alongshore averaged manifestation of the slight meandering nature of the Benguela Current: the positive contribution to vorticity by the tadv term drives a poleward transport component, which is consistent with the slightly less negative beta term at this location.

In the REF simulation the wind stress curl, beta effect, vortex stretching, and total advection terms are all significant. The vstretch term becomes particularly important offshore of 400 km from the coast, which is coincident with the second "stream" of the Benguela Current that is thought to be the mean manifestation of the preferential passage of Agulhas Rings. The large positive vstretch term in this region is connected with the anticyclonic Agulhas Rings and introduces a positive source of vorticity that is consistent with the equatorward advection of the rings (which is reflected in the large, negative beta term). The total advection term associated with the passage of Agulhas Rings is not dominated by the eddy component; rather over the 400–550 km offshore region, the mean and eddy advection components undulate so that they are more or less equal. This is consistent with the work of *Treguier et al.* [2003] who emphasized that the dominance of anticyclonic rings as opposed to cyclonic eddies does not allow for the transient component of flow to be entirely removed from the mean state. Closer inshore, from about 250 to 400 km, the eddy component of the total advection term dominates, suggesting the presence of small scale instabilities of features associated with the upwelling front and their interaction with mesoscale features Agulhas leakage. In the vicinity of the shelf-edge at about 220 km offshore, as in the NOA experiment, the vstretch and tadv terms dominate due to the alongshore advection of the cyclonic, shelf-edge eddies.

At the shelf-edge in both simulations, though much more intense in the REF simulation, is a positive spike in the vstretch term. This is consistent with vortex squashing and the upward vertical velocities seen in Figure 9 as the equatorward current moves over the shelf-edge where its height is decreased.

4. Conclusions

The difficulty of removing the signal of the Agulhas from the Benguela is well known. Unequivocal conclusions on the role of the Agulhas in the Benguela system are therefore similarly difficult to achieve. The use of numerical models allows us to purposefully create unrealistic scenarios in order to investigate the dominant driving forces of particular features. By introducing a dam at ∼30°S on the east coast in the model, we cause an early retroflection of the Agulhas Current such that its influence on the Benguela system is minimal. Comparisons of this simulation (NOA) with the realistic one (REF), which has the same configuration and forcing, has allowed for some conclusions to be made on the role of the Agulhas Current in the Benguela system.

The most distinctive and expected effect of the Agulhas on the southern Benguela system is the warm water that it introduces. The fact that the warming effect is greatest in the offshore region and least on the shelf means that it has an intensifying effect on the thermal front across the shelf-edge in the southern Benguela and therefore also on the associated jet currents. The offshore extent and generation of filaments is further limited by the high level of turbulence introduced by Agulhas leakage causing intense mixing and diffusion beyond the shelf-edge. The geostrophically adjusted equatorward current that is intensified by Agulhas influx in the vicinity of the shelf-edge in the southern Benguela results in dynamic uplift at the shelf-edge, which brings cooler and fresher water to the surface. North of about 30°S the effect of the Agulhas on the upwelling front is less, but the large filaments at Lüderitz (about 28°S) are present in both the REF and NOA simulations as is the associated region of high surface EKE linked with frontal instabilities there. This suggests that the filaments are not dependent on interaction with Agulhas Rings for their huge offshore expanse but are rather a result of the perennial nature of the upwelling-favorable wind in conjunction with the large-scale offshore geostrophic flow in the vicinity of Lüderitz.

Analysis of the large-scale transport of the region from both simulations reveals that while the Agulhas contributes about 15 Sv to the Benguela transport (which is consistent with other results [e.g., *Reason et al.*, 2003; *Matano and Beier*, 2003; *van Sebille et al.*, 2010; *Doglioli et al.*, 2006; *Biastoch et al.*, 2008b], a large portion of it is in the form of dominantly large anticyclonic (as opposed to cyclonic) eddies that are difficult to remove from the mean signal. This is suggested by the fact that the corridor of Agulhas Rings exists in the region of greatest mean transport and highest surface EKE. The vorticity budget explicitly shows that without the influence of the extreme nonlinearities associated with Agulhas influx the Sverdrup balance holds in the offshore domain. It also shows that while the eddy component of the total advection term dominates within about 200 km of the shelf-edge, presumably due to instabilities associated with the interaction of Agulhas influx and shelf-edge features, beyond that it is more or less split between the eddy and mean components. The latter finding is consistent with the location of the corridor of large-scale eddies as well as the idea that the signal of the large-scale eddies are difficult to separate from the mean state. The very high EKE introduced by Agulhas influx exists in the offshore domain of the southern Benguela, rapidly dissipating in the vicinity of the shelf-edge, suggesting that high turbulence associated with the Agulhas does not directly influence the ecologically important southern Benguela shelf. However, there exists high variability on the narrow shelf and shelf-edge between Cape Point to just north of Cape Columbine in both REF and NOA simulations. This is associated with the intense temperature gradients, alongshore jet and associated baroclinic instabilities present with or without the Agulhas.

Over the shelf and shelf-edge region, the Agulhas has an important role to play in the generation of an intense geostrophic shelf-edge jet that produces dynamic uplift at the shelf-edge via vortex squashing. More specifically, it intensifies and broadens the Good Hope Jet by enhancing the cross-shelf steric-height gradient via the injection of warm offshore waters. The Good Hope Jet exists in the NOA experiment via the density gradients introduced during active upwelling and is somewhat enhanced by the narrow shelf in the region. However, it is a more strongly seasonal feature, rather than perennial, without the Agulhas influence.

While this numerical modeling experiment does not remove the effect of the Agulhas entirely (i.e., the boundary conditions and the surface restoring term both retain the signal of Agulhas waters), it has allowed us to make some inferences on the effect of Agulhas leakage on the mean state of the Benguela system. It has shown that the Agulhas not only significantly affects the large-scale flow regime but also impacts nearshore features which can have critical ramifications for the health of the southern Benguela ecosystem.

References

Bang, N., and W. Andrews (1974), Direct current measurements of a shelf-edge frontal jet in the southern Benguela system, *J. Mar. Res.*, *32*, 405–417.

Biastoch, A., C. Boning, and J. Lutjeharms (2008a), Agulhas leakage dynamics affects decadal variability in Atlantic overturning circulation, *Nature*, *456*(7221), 429–436.

Biastoch, A., J. Lutjeharms, C. Bönning, and M. Scheinert (2008b), Mesoscale perturbations control inter-ocean exchange south of Africa, *Geophys. Res. Lett.*, *35*, L20602, doi:10.1029/2008GL035132.

Boebel, O., J. Lutjeharms, C. Schmid, W. Zenk, T. Rossby, and C. Barron (2003), The Cape Cauldron: A regime of turbulent inter-ocean exchange, *Deep Sea Res., Part II*, *50*, 57–86.

Capet, X., F. Colas, P. Penven, P. Marchesiello, and J. McWilliams (2008), Eddies in eastern boundary subtropical upwelling systems, in *Ocean Modeling in an Eddying Regime*, vol. 177, AGU, Washington, D. C.

Chang, N. (2009), Numerical ocean model study of the Agulhas Bank and the Cool Ridge, PhD thesis, Univ. of Cape Town, Cape Town, South Africa.

Chelton, D., R. deSzoeke, and M. Schlax (1998), Geographical variability of the first Rossby radius of deformation, *J. Phys. Oceanogr.*, *28*, 433–460.

Conkright, M., R. Locarnini, H. Garcia, T. O'Brien, T. Boyer, C. Stephens, and J. Antonov (2002), World Ocean Atlas 2001: Objective analyses, data statistics and figures, CR-ROM documentation, *Inter. Rep. 17*, Natl. Oceanogr. Cent., Silver Spring, Md.

Da Silva, A., C. Young, and S. Levitus (1994), Atlas of surface marine data 1994: Algorithms and procedures, technical report, vol. 1, Natl. Oceanogr. and Atmos. Admin., Silver Spring, Md.

Debreu, L., C. Voulard, and E. Blayo (2008), AGRIF: Adaptive grid refinement in fortran, *Comput. Geosci.*, *34*, 8–13.

Debreu, L., P. Marchesiello, P. Penven, and G. Cambon (2012), Two-way nesting in split-explicit ocean models: Algorithms, implementation and validation, *Ocean Modell.*, *49–50*, 1–21.

de Ruijter, W., A. Biastoch, S. Drijfhout, J. Lutjeharms, R. Matano, T. Pichevin, P. van Leeuwen, and W. Weijer (1999), Indian-Atlantic inter-ocean exchange: Dynamics, estimation and impact, *J. Geophys. Res.*, *104*(C9), 20,885–20,910.

Doglioli, A., M. Veneziani, B. Blanke, S. Speich, and A. Griffa (2006), A Lagrangian analysis of the Indian-Atlantic interocean exchange in a regional model, *Geophys. Res. Lett.*, *33*, L14611, doi:10.1029/2006GL003952.

Duncombe-Rae, C., F. Shilington, J. Agenbag, J. Taunton-Clark, and M. Grundlingh (1992), An Agulhas ring in the south Atlantic ocean and its interaction with the Benguela upwelling frontal system, *Deep Sea Res., Part I*, *39*(11/12), 2009–2027.

Durgadoo, J., B. Loveday, C. Reason, P. Penven, and A. Biastoch (2013), Agulhas leakage predominantly responds to the Southern Hemisphere Westerlies, *J. Phys. Oceanogr.*, *43*, 2113–2131.

Garzoli, S., and A. Gordon (1996), Origins and variability of the Benguela Current, *J. Geophys. Res.*, *101*(C1), 897–906.

Garzoli, S., A. Gordon, V. Kamenkovich, D. Pillsbury, and C. Duncombe-Rae (1996), Variability and sources of the southeastern Atlantic circulation, *J. Mar. Res.*, *54*, 1029–1071.

Gordon, A. (2003), The brawniest retroflection, *Nature*, *421*, 904–905.

Gruber, N., Z. Lachkar, H. Frenzel, P. Marchesiello, M. Münnich, J. McWilliams, T. Nagai, and G.-K. Plattner (2011), Eddy-induced reduction of biological production in eastern boundary upwelling systems, *Nat. Geosci.*, *4*, 787–792.

Haidvogel, D., and A. Beckmann (1999), *Numerical Ocean Modeling, Environ. Sci. Manage.*, vol. 2, Imperial College Press, London.

Large, W., J. McWilliams, and S. Doney (1994), Oceanic vertical mixing: A review and a model with a nonlocal boundary layer parameterization, *Rev. Geophys.*, *32*(4), 363–403.

Loveday, B., J. Durgadoo, C. Reason, A. Biastoch, and P. Penven (2014), Decoupling of the Agulhas leakage from the Agulhas Current, *J. Phys. Oceanogr.*, *44*(7), 1776–1797.

Loveday, B., P. Penven, and C. Reason (2015), Southern annular mode and westerly-wind driven changes in Indian-Atlantic exchange mechanisms, *Geophys. Res. Lett.*, *42*, 4912–4921, doi:10.1002/2015GL064256.

Lutjeharms, J., and C. Mathyssen (1995), A recurrent eddy in the upwelling front off Cape Town, *S. Afr. J. Sci.*, *91*(7), 355–357.

Lutjeharms, J., and P. Stockton (1987), Kinematics of the upwelling front off Southern Africa, in *The Benguela and Comparable Ecosystems*, edited by A. Payne, J. Gullard, and K. Brink, *S. Afr. J. Mar. Sci*, pp. 35–49.

Lutjeharms, J., F. Shillington, and C. M. Rae (1991), Observations of extreme upwelling filaments in the southeast Atlantic Ocean, *Science*, *253*, 774–776.

Marchesiello, P., J. McWilliams, and A. Schepetkin (2001), Open boundary conditions for long-term integration of regional oceanic models, *Ocean Modell.*, *3*, 1–20.

Marchesiello, P., J. McWilliams, and A. Schepetkin (2003), Equilibrium structure and dynamics of the California Current system, *J. Phys. Oceanogr.*, *33*, 753–783.

Marchesiello, P., L. Debreu, and X. Couvelard (2009), Spurious diapycnal mixing in terrain-following coordinate models: The problem and a solution, *Ocean Modell.*, *26*(3–4), 156–169, doi:10.1016/j.ocemod.2008.09.004.

Matano, R., and E. Beier (2003), A kinematic analysis of the Indian/Atlantic interocean exchange, *Deep Sea Res., Part II*, *50*, 229–249.

Nelson, G. (1985), Notes on the physical oceanography of the Cape Peninsula upwelling system, in *South African Ocean Colour and Upwelling Experiment*, edited by L. V. Shannon, pp. 63–95, Sea Fisheries Research Institute, Cape Town.

Nelson, G., and L. Hutchings (1983), The Benguela upwelling area, *Prog. Oceanogr.*, *12*(3), 333–356.

Penven, P., V. Echevin, J. Pasapera, F. Colas, and J. Tam (2005), Average circulation, seasonal cycle, and mesoscale dynamics of the Peru Current system: A modelling approach, *J. Geophys. Res.*, *110*, C10021, doi:10.1029/2005JC0029.

Penven, P., L. Debreu, P. Marchesiello, and J. McWilliams (2006a), Evaluation and application of the ROMS 1-way embedding procedure to the central California upwelling system, *Ocean Modell.*, *12*, 157–187.

Penven, P., J. Lutjeharms, and P. Florenchie (2006b), Madagascar: A pacemaker for the Agulhas Current system?, *Geophys. Res. Lett.*, *33*, L17609, doi:10.1029/2006GL026854.

Penven, P., P. Marchesiello, L. Debreu, and J. Lefevre (2007), Software tools for pre- and post-processing of oceanic regional simulations, *Environ. Modell. Software*, *23*, 660–662, doi:10.1016/j.envsoft.2007.07.004.

Peterson, R., and L. Stramma (1991), Upper-level circulation in the South Atlantic, *Prog. Oceanogr.*, *26*, 1–73.

Reason, C., J. Lutjeharms, J. Hermes, A. Biastoch, and R. Roman (2003), Inter-ocean fluxes south of Africa in an eddy-permitting model, *Deep Sea Res., Part II*, *50*(2), 281–298.

Richardson, P. (2007), Agulhas leakage into the Atlantic estimated with subsurface floats and surface drifters, *Deep Sea Res., Part I*, *54*(8), 1361–1389.

Rossi, V., C. Lopez, J. Sudre, E. Henandez-Garcia, and V. Garcon (2008), Comparative study of mixing and biological activity of the Benguela and Canary upwelling systems, *Geophys. Res. Lett.*, *35*, L11602, doi:10.1029/2008GL033610.

Rubio, A., B. Blanke, S. Speich, N. Grima, and C. Roy (2009), Mesoscale eddy activity in the southern Benguela upwelling system from satellite altimetry and model data, *Prog. Oceanogr.*, *83*, 288–295.

Schouten, M., W. de Ruijter, P. van Leeuwen, and J. Lutjeharms (2000), Translation, decay and splitting of Agulhas rings in the southeastern Atlantic Ocean, *J. Geophys. Res.*, *105*(C9), 21,913–21,925.

Shannon, L., and G. Nelson (1996), The Benguela: Large-scale features and processes and system variability, in *The South Atlantic: Present and Past Circulation*, pp. 163–210, Springer, Berlin.

Shchepetkin, A., and J. McWilliams (2008), Computational kernel algorithms for fine-scale, multi-process, long-term oceanic simulations, *Handb. Numer. Anal.*, *14*, 119–181.

Shchepetkin, A., and J. McWilliams (1998), Quasi-monotone advection schemes based on explicit locally adaptive dissipation, *Mon. Weather Rev.*, *126*, 1541–1580.

Shchepetkin, A., and J. McWilliams (2005), The regional oceanic modeling system (ROMS): A split-explicit, free-surface, topography-following-coordinate oceanic model, *Ocean Modell.*, *9*, 347–404.

Shchepetkin, A., and J. McWilliams (2008), Computational kernel algorithms for fine-scale, multi-process, long-term oceanic simulations, in *Handbook of Numerical Analysis: Computational Methods for the Ocean and Atmosphere*, pp. 119–181, Elsevier Sci.

Shelton, P., and L. Hutchings (1982), Transport of anchovy, Engraulis capensis Gilchrist, eggs and early larvae by a frontal jet current, *ICES J. Mar. Sci.*, *40*, 185–198.

Shillington, F., W. Peterson, L. Hutchings, T. Probyn, H. Waldron, and J. Agenbag (1990), A cool upwelling filament off Namibia, southwest Africa: Preliminary measurements of physical and biological features, *Deep Sea Res., Part A*, *37*(11), 1753–1772.

Soufflet, Y., P. Marchesiello, F. Lemari, J. Jouanno, X. Capet, L. Debreu, and R. Benshila (2016), On effective resolution in ocean models, *Ocean Modell.*, *98*, 36–50, doi:10.1016/j.ocemod.2015.12.004.

Strub, P., F. Shillington, C. James, and S. Weeks (1998), Satellite comparison of the seasonal circulation in the Benguela and California Current systems, in *Benguela Dynamics*, vol. 19, edited by S. Pillar et al., *S. Afr. J. Mar. Sci.*, pp. 99–112.

Treguier, A., O. Boebel, B. Barnier, and G. Madec (2003), Agulhas eddy fluxes in a 1/6 degree Atlantic model, *Deep Sea Res., Part II*, *50*, 251–280.

van Aken, H. V., J. Lutjeharms, M. Rouault, C. Whittle, and W. de Ruijter (2013), Observations of an early Agulhas current retroflection event in 2001: A temporary cessation of inter-ocean exchange south of Africa?, *Deep Sea Res., Part I*, *72*, 1–8.

van Foreest, D., F. Shillington, and R. Legeckis (1984), Large scale, stationary, frontal features in the Benguela Current system, *Cont. Shelf Res.*, *3*(4), 465–474.

van Sebille, E., P. van Leeuwen, A. Biastoch, and W. de Ruitjer (2010), Flux comparison of Eulerian and Lagrangian estimates of Agulhas leakage: A case study using a numerical model, *Deep Sea Res., Part I*, *57*, 319–327.

Veitch, J., P. Penven, and F. Shillington (2009), The Benguela: A laboratory for comparative studies, *Prog. Oceanogr.*, *83*, 296–302, doi: 10.1016/j.pocean.2009.07.008.

Veitch, J., P. Penven, and F. Shillington (2010), Modeling equilibrium dynamics of the Benguela Current system, *J. Phys. Oceanogr.*, *40*, 1942–1963.